Physics Letters A 379 (2015) 2351–2356

Contents lists available at ScienceDirect

Physics Letters A

www.elsevier.com/locate/pla

On mechanisms of choked gas flows in microchannels

Xiaodong Shan, Moran Wang *

Department of Engineering Mechanics and CNMM, Tsinghua University, Beijing 100084, China

ARTICLE INFO

Article history:
Received 13 April 2015
Received in revised form 22 July 2015
Accepted 25 July 2015
Available online 29 July 2015
Communicated by R. Wu

Keywords:
Choked gas flows
Effective pressure ratio
GEMC
Subsonic choking

ABSTRACT

Choked gas flows in microchannels have been reported before based solely on experimental measurements, but the underlining physical mechanism has yet to be clarified. In this work, we are to explore the process via numerical modeling of choked gas flows through a straight microchannel that connects two gas reservoirs. The major theoretical consideration lies in that, since the gas in microchannels may not be necessarily rarefied even at a high Knudsen number, a generalized Monte Carlo method based on the Enskog theory, GEMC, was thus used instead of direct simulation Monte Carlo (DSMC). Our results indicate that the choked gas flows in microchannels can be divided into two types: sonic choking and subsonic choking, because the sonic point does not always exist even though the gas flows appear choked, depending on the inlet–outlet pressure ratio and the length–height ratio of the channel. Even if the gas flow does not reach a sonic point at the outlet region, the effective pressure ratio (p_i/p_o) acting on the channel becomes asymptotically changeless when the pressure ratio on the buffer regions (p_i'/p_o') is higher than a certain value. The subsonic choking may caused by the expansion wave or the strong non-equilibrium effect at the outlet.

1. Introduction

In the past two decades, developments of MEMS/NEMS technologies have enabled us to fabricate various microfluidic or nanofluidic devices [1–4] with unique functions such as sensing, cooling and actuating. Especially the gas microfluidics, including micro nozzles [5–7], micro gas flowmeters [8,9] and other micro-metering gas sensors [8,10], have attracted more and more attention owing to their distinctive capabilities and applications. Recently, the gas percolation mechanism in nano-pores requires urgent demands because of tight gas reservoir or shale gas recovery and developments [11,12]. Therefore, a better and accurate understanding of the mechanisms of gas flow and heat transfer in microchannels and nanochannels is very important and critical for design and analysis of micro- and nanosystems [3,4]. The previous studies have reported some special characteristics of gas flow and heat transfer in micro- and nanochannels at high Knudsen number [13–29]. When the gas density is sufficiently low so that it can be treated as ideal gas, the micro gas flow shows similar behaviors as rarefied gas, including flow slip and temperature jump on surfaces [30]; if the gas is so dense however that the assumption of ideal gas breaks down, the non-ideal gas effect will influence the flow resistance and heat transfer on surfaces [16,22]. Such non-ideal gas flow in microchannels renders a direct challenge to the conventional theories and it is therefore crucial to study the new physics and clarify the mechanisms in such flow and heat transfer processes.

As well known, in the classical gas dynamics, when the inlet–outlet pressure ratio reaches certain value, gas flow in a channel at continuum scale (i.e. $\mathrm{Kn} \ll 1$), either variable cross-section or a straight one, will be choked because of the occurrence of the sonic point, at the throat position for the variable cross-section nozzle or at the center of exit for the straight channel [31]. However, experimental studies have demonstrated that gas flows driven by a pressure difference through microchannels behave differently from such classical theories [6,17,24,32]. For micro-nozzles with variable cross sections, once the gas flow is choked, the sonic point moves backwards from the throat due to the higher viscous dissipation at smaller cross section [6]. For straight microchannels, both experiments and numerical simulations have reported other anomalous behaviors of choked gas flows [17,32]. For instance, Yao et al. [17] found through experiments that when the inlet–outlet pressure ratio reached a critical value in a long straight microchannel connecting two gas reservoirs, the mass flow rate became constant, and meanwhile the outlet Mach number was found below 1. They called such phenomenon as *subsonic* choked gas flow, and ascribed it to a general "surface effects" [6,17]. Consequently, a numerical modeling was conducted, using the direct simulation Monte Carlo (DSMC) method, of a straight microchannel (without reservoirs), and the results showed that the sonic point still appeared

* Corresponding author. Tel.: +86 10 627 87498.
E-mail address: mrwang@tsinghua.edu.cn (M. Wang).

http://dx.doi.org/10.1016/j.physleta.2015.07.036
0375-9601/

when gas choked but only around a small area at the outlet, thus leading the averaged velocity across the channel into the subsonic regime [33]. However, the mechanisms of small-area-sonic-point cannot explain the choking appearance for long channels when the sonic point never appears. One the other side, theoretical studies have indicated that the mass flux in a long microchannel driven by finite pressure difference approaches its minimum when the Knudsen number is around 1. Yet, no theories are available to explain the subsonic choked gas flow at small Knudsen numbers in the previous experiments.

In this present work, the mechanism of choked gas flows in straight microchannels is investigated using numerical simulations. Considering the greater surface friction in microchannels than that in conventional channels, a Monte Carlo method based on the Enskog theory for dense gases which thus has a broader capability than the direct simulation Monte Carlo (DSMC) method is used for the high-density high-Kn gas flows. To explore the physics of the anomalous choking in microchannel gas flows, the existence of sonic point, the unique feature in such cases, is examined by considering the effects of rarefaction, pressure distribution or propagation of pressure waves, and surface friction.

2. Methods

Since the inlet pressure usually has to be sufficiently high to overcome the high surface friction and to drive the gas flowing through the microchannel, the gas density will change gradually from high (dense) to low (rarefied) [17]. At the same time, the tiny characteristic length in the microchannel leads to a high Knudsen number, even at the high densities of gas. The temperature also drops drastically near the exit of the channels due to gas expansion into even lower ambient pressure [5]. Consequently both assumptions of rarefied gas and ideal gas, the important foundations for conventional theories, will break down in these cases [16]. In this work, a Monte Carlo method based on the Enskog equation, thus termed the generalized Enskog Monte Carlo method (GEMC) [34], is adopted to simulate the gas flows in a straight microchannel.

The GEMC method is developed for non-ideal gas by considering the high-density effect on collision rates, and for a Lennard-Jones fluid, by including both repulsive and attractive molecular interactions. By means of the Enskog theory, the enhanced collision rate can be determined with the excluded molecular volume and the shadowing/screening effects. Furthermore, the internal energy exchange model is also developed based on the Parker's formula [35], to work with the generalized collision model [34–36]. Therefore the equation of state for a non-ideal gas is derived from the Clapeyron equation to the van der Waals equation by considering the finite density effect and van der Waals intermolecular force [34]. GEMC has been proved valid for both ideal and non-ideal gas flow and associated heat transfer [22], and is suitable for a wide temperature region [34]. When the gas is at a low density, GEMC will degrade to DSMC. Similar to DSMC [37], GEMC requires the cell size smaller than the mean free path of the gas molecules and the computational time step less than the mean collision time, to ensure the accuracy of simulation results.

In the previous experiments [17], the microchannel connecting two gas chambers, the pressure of each chamber was kept at a different yet fixed value, and the gas was driven through the microchannel by the pressure difference. To compare with their experimental results, we added two identical buffer regions at ends of the microchannel in our model shown in Fig. 1, and set the walls temperature at 300 K. Two chosen pressures, p_i' and p_o', are given to the buffer regions [38], and for simplicity without losing the generality, we actually designate the outlet pressure to reduce gradually to vacuum in our simulations. The actual inlet and outlet pressures, p_i and p_o, i.e., the effective pressure ratio (p_i/p_o), acting on the microchannel, are related to the geometries of channel and the boundary conditions and determined from the simulations. The microchannel is L in length and H in height. The channel height (H) is typically set 0.1 micron in the following cases, and may vary from 0.01 to 1 micron depending on requirement of Kn variations. The buffer zone is $3H$ in height and $L_b = H$ in length, or the length–height ratio $s = L/H = 3$. Prior to simulation, we first checked size effect of buffer zones by altering their dimensions, and no noticeable difference in the results was found, as long as both buffer zones remain identical in shape and in ratio s. However, the predictions changed significantly if no buffer zones were attached. Also in our simulation, the length–height ratio s of the microchannel, which impacts the surface resistance to the gas flow, is altered to check its effect.

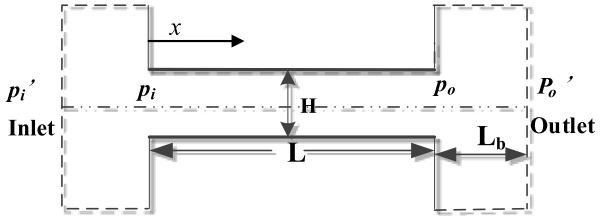

Fig. 1. The geometry of microchannel with reservoir zones at both ends. The channel is L long and H high. The inlet and outlet pressure in the reservoirs are p_i' and p_o', and the pressure actually acting on the channel inlet and outlet are p_i and p_o.

3. Simulation results and discussions

In our simulation, by varying the outlet pressure p_o' for a given inlet pressure p_i', we pay attention to two key dimensionless parameters: the inlet–outlet pressure ratio (p_i'/p_o') and the length–height ratio (s). To demonstrate the validity of our model, we run the simulation on a short microchannel $(s = 5)$ which has been adapted by other studies [33], just to detect the occurrence of sonic or subsonic choked flows by changing the inlet pressure (p_i') from 0.01 to 0.5 MPa. The influence of the surface friction on the gas choking behaviors in microchannel is then studied by switching the length–height ratio(s) from 5, 10, 15, 20, 30 to 40 for a given inlet pressure p_i'. The results are illustrated and discussed as follows.

3.1. Sonic and subsonic choking

In comparison to the previous numerical simulations [33] on gas flow in a short microchannel driven by an inlet pressure at 1 atm, the case with $s = 5$ and $p_i' = 0.1$ MPa is repeated as the first step. The pressure contour calculated is shown in Fig. 2(a), indicating that the distribution of pressure in the same cross-section of channel is non-uniform, especially at the boundaries with a dramatic change in the outlet buffer region: thus the pressures referred to hereafter are all the mean values of the corresponding cross sections.

Fig. 2(b) on the other hand offers the non-dimensional flow rate normalized by that with a vacuum outlet, as a function of the inlet–outlet pressure ratio (p_i'/p_o') at 3 given levels of inlet pressure p_i'. The flow rate increases with p_i'/p_o' and approaches asymptotically to 1. Although a higher given p_i' value leads to a greater initial flow rate, the 3 curves at different p_i' values converge when p_i'/p_o' reaches respectively from 20 to 50. When the flow rate is no longer increasing with the elevating pressure p_i'/p_o', the gas flow is choked.

Fig. 2(c) shows the distributions of real pressure along the channel length for different buffer inlet–outlet pressure ratios (p_i'/p_o') at $p_i' = 0.1$ MPa. The result indicates that when p_i'/p_o' is higher than 20, the real pressure profiles along the channel roughly

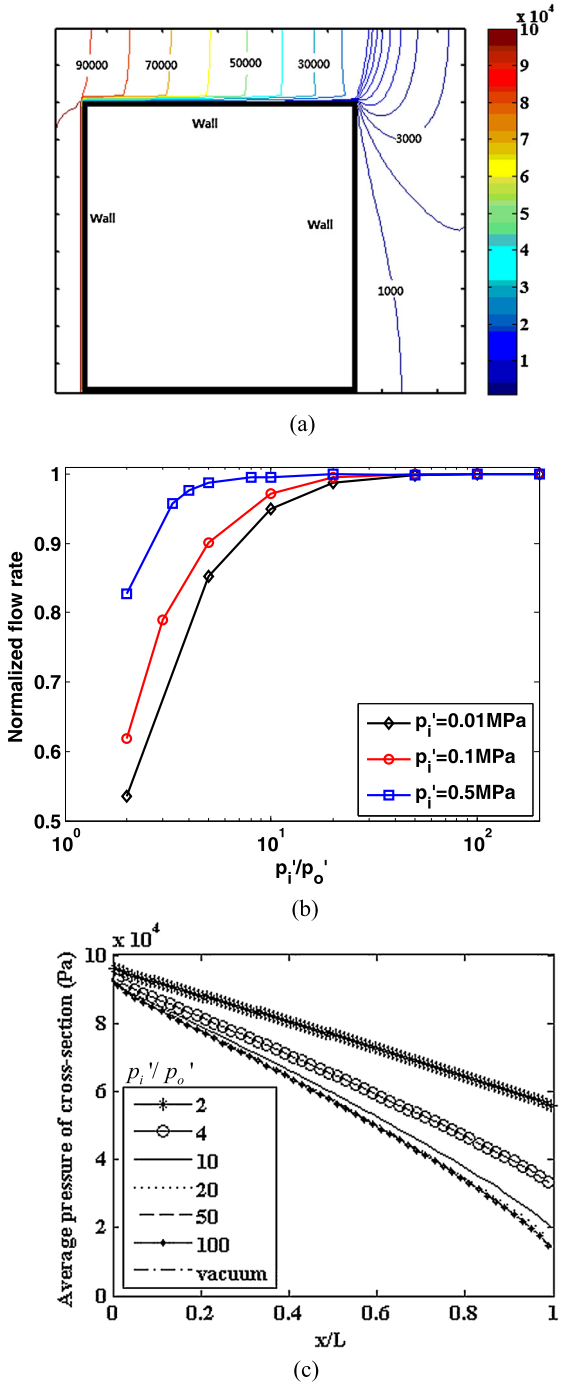

Fig. 2. (a) Pressure contour in the computational domain for inlet pressure as 1 atm and outlet pressure as vacuum. (b) Normalized mass flow rate versus the given inlet–outlet pressure ratio at buffers for three different inlet pressures (0.01, 0.1 and 0.5 MPa). The flow rate is normalized by its maximum when vacuum at outlet. The length–height ratio $s = 5$ in these simulations. (c) Distributions of average pressure of cross-section along the channel for different p_i'/p_o'. The inlet pressure is assigned as 0.1 MPa, the channel height is 0.1 μm and the inlet Kn is about 0.7.

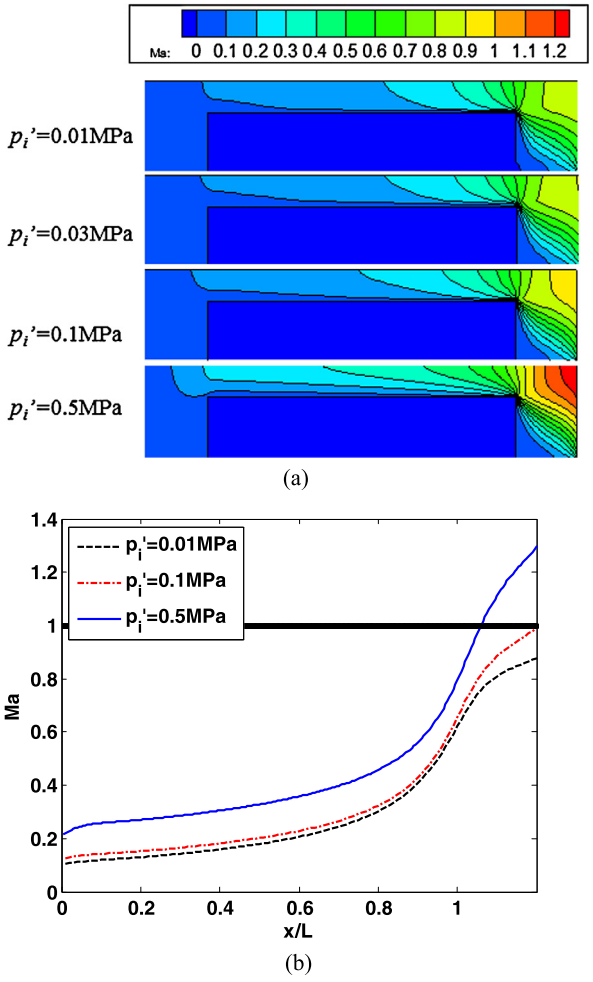

Fig. 3. Mach number distributions for different given inlet pressures. (a) Mach contours for four given inlet pressure, $p_i' = 0.01$, 0.03, 0.1 or 0.5 MPa, when vacuum at outlet. The maximum Mach number is 0.88, 0.9062, 0.99 and 1.3 respectively. (b) Mach number profiles along the centerline of channel for three inlet pressure, $p_i' = 0.01$, 0.1 or 0.5 MPa. The reference line is Ma = 1.

coincide, i.e. not recognized from each other anymore. This means that the pressure field actually acting on the channel is changeless for high p_i'/p_o'. In other word, the gas flow appears choked. Similar choking occurs for a higher inlet pressure ($p_i' = 0.5$ MPa) or a lower inlet pressure ($p_i' = 0.01$ MPa), as shown in Fig. 2(b). Different inlet pressure (p_i') corresponds to different critical values of p_i'/p_o' when choking starts.

Another interesting issue to us is to check the Mach number. Fig. 3(a) shows our simulated Mach contours are shown in Fig. 3(a) and the Mach number profiles along the centerline of channel are compared in Fig. 3(b) for different inlet pressures p_i'. Note that Fig. 2 has already indicated that in all of these cases, the gas flows are choked. The results in Fig. 3 show that, even though the gas flows are choked, the sonic area or point is not achieved in the microchannel, which is different from the previous result [16]. In other words the appearance of sonic point is not necessary for gas choking in microchannel and gas flows may be choked at both subsonic and sonic speeds. For fear of changing physics, we divide all the choked gas flows into two types: sonic choking and subsonic choking. In sonic choking, the compressibility of gas plays the key role based on the classical gas dynamics; while in subsonic choking, the mechanism may be different and will be discussed in the next section.

3.2. Effective pressure ratio

As well known in classical gas dynamics, for gas flow driven by a pressure difference in a straight channel, if the given pressure drop is higher than the critical value, the gas may be accelerated to the sonic speed at outlet and adjust the effective pressure drop by itself based on compressibility. In other word, the effective pressure drop may differ from the given pressure difference. Inspired by this, we check the effective pressure ratios versus the given pressure ratios for both sonic and subsonic choked gas flows

in microchannels. Fig. 4 shows the results for different given inlet pressure in a microchannel with a length–height ratio $s = 5$. The case of $p_i' = 0.1$ MPa is used as a reference one for both Fig. 4(a) and 4(b) because it happens to reach the sonic point (Ma ≈ 1 in very small area in the middle of channel) at the outlet, which has been indicated in Fig. 3(b). Therefore the effective pressure ratios in Fig. 4(a) are for subsonic gas choking and those in Fig. 4(b) are for sonic choking.

In our simulations, the pressure ratio p_i'/p_o' is increased by reducing the outlet pressure p_o' for a given inlet pressure p_i'. The results in both figures (4(a) and 4(b)) indicate that when p_i'/p_o' is not too high, the effective pressure ratio p_i/p_o rises with p_i'/p_o'. When the outlet pressure p_o' gets lower than a certain value (p_i'/p_o' larger than a value), the no matter how the gas gets choked, it is very interesting to find that the effective pressure ratio (p_i/p_o) acting on the channel becomes asymptotically changeless for a given inlet pressure, as shown in Fig. 4(a and b). In other word, when the pressure ratio on buffer regions is large enough and keep increasing, the effective pressure ratio will only mount with infinitesimal to approach the value at a vacuum outlet. This may be the main phenomenal cause of gas choked for large given pressure ratios. The asymptotical effective pressure ratios are different for subsonic or sonic gas choked flows. For the subsonic gas choking, as shown in Fig. 4(a), these ratios look close for different inlet pressures p_i'. The lower is p_i', the closer are the ratios. The sonic gas choking is quite different as shown in Fig. 4(b). The asymptotical effective pressure ratios vary significantly with the inlet pressures. The higher is p_i', the lower is the ratio. In fact, it is the existence of buffer region in the outlet region, which is necessary compared with experiments, that leads to this asymptotical change.

The pressure drop is to drive the gas flow in the channel, overcoming surface resistance, and to accelerate the flow to higher speed if possible. For sonic choked flows, the flow compressibility plays the key role to adjust the pressure distribution in the channel. For the subsonic choking, the mechanism is different. As known that the surface resistance increases sensitively with the gas flow speed in the channel. For a given high pressure drop between reservoirs, the gas actually compromises between expansion-acceleration and speed-up-resistance-rising. The effective pressure distribution acting on the channel is therefore reformed according to the balance between the driving force and the surface and inertial resistance. No theories up to now can perfectly explain the significant pressure drop from the channel outlet (p_o) to the reservoir (p_o') for a subsonic gas flows. Yet the NASA report [39] found that an expansion wave may form and propagate pressure information even in subsonic gas flows. Although the expansion wave has not been caught in our simulations, it is reasonable to believe that it is the expansion wave downstream the channel outlet that holds the effective pressure ratio (p_i/p_o) when the outlet pressure p_o' decreases lower than the critical value. A recent experiment and analysis on expansion wave of rarefied gas flow confirms our suspicion on the role of expansion wave for reforming the pressure at the outlet region [40,41]. Further studies are still necessary to discover the mechanism of expansion wave in subsonic flows. Meanwhile the strong non-equilibrium effect at outlet may play another key role because the Knudsen number at outlet is very high generally.

3.3. Length–height ratio

As stated above, the surface friction plays an important role in choked gas flows in microchannel. A recent study has shown that the length–height ratio of channel dominates the effective resistance of gas flows in microchannels [29]. In this contribution, we model the choked gas flows in microchannels with different length–height ratios driven by a given inlet pressure p_i' to vacuum. The channel height is fixed and the length is changable. Fig. 5(a) shows the Mach number distributions of choked gas flows along the centerline of the channel for different lengths. As the microchannel becomes longer for a given inlet pressure, the maximum of Mach number in the flow may drop from unity to smaller, and the choked flows can degrade from sonic choking to subsonic choking. It means that the length–height ratio may change the choking pattern of gas flows in microchannels.

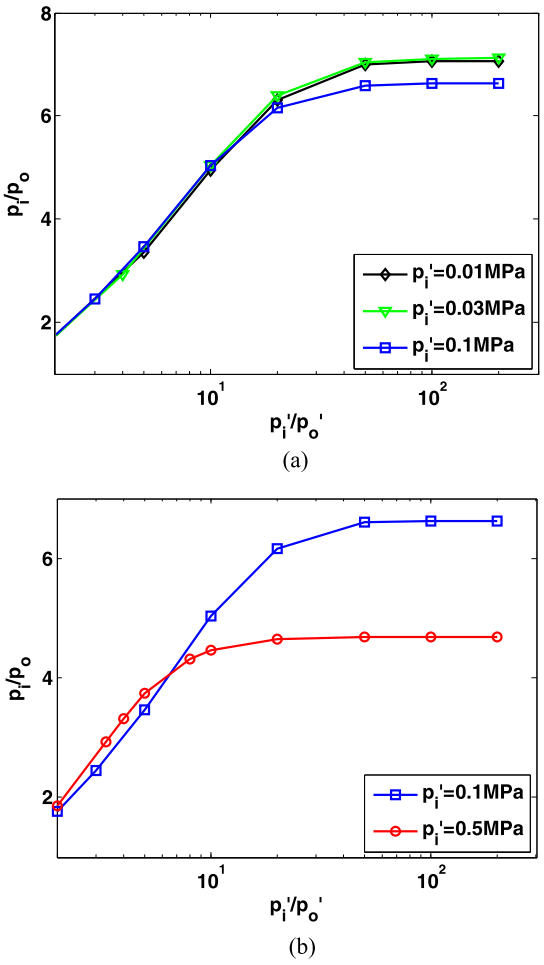

Fig. 4. The effective pressure ratio, p_i/p_o, acting on microchannel versus the given pressure ratio, p_i'/p_o', at buffer inlet and outlet for different inlet pressure, p_i' (a) for subsonic choked gas flows; (b) for sonic choked flows. The case of $p_i' = 0.1$ MPa is used as a reference one for both cases because it happens to have a Ma $= 1$ at the outlet for the microchannel with $s = 5$.

It is known from Fig. 4 that the effective pressure ratio (p_i/p_o) acting on the channel becomes asymptotically changeless for a given inlet pressure when the pressure ratio on the buffer regions (p_i'/p_o') is high enough. The asymptotical effective pressure ratio p^*_{asym} can be accurately calculated by assigning the outlet boundary condition as vacuum for a given p_i'. It is clear that p^*_{asym} highly depends on the surface friction and therefore on the length–height ratio (s). Fig. 5(b) shows the relationship between p^*_{asym} and s, which appears linear. A fitting line is also plotted in the same figure and the coefficient of determination $R^2 = 1$ means the linearity is perfect for this case. This linear response between the balanced effective pressure ration p^*_{asym} and the channel length means that the surface friction plays the key role in the subsonic choked gas flow in microchannels. It should be noted that when length height ratio is large enough, 100 for example, this linear behavior may not hold any more by our further simulations.

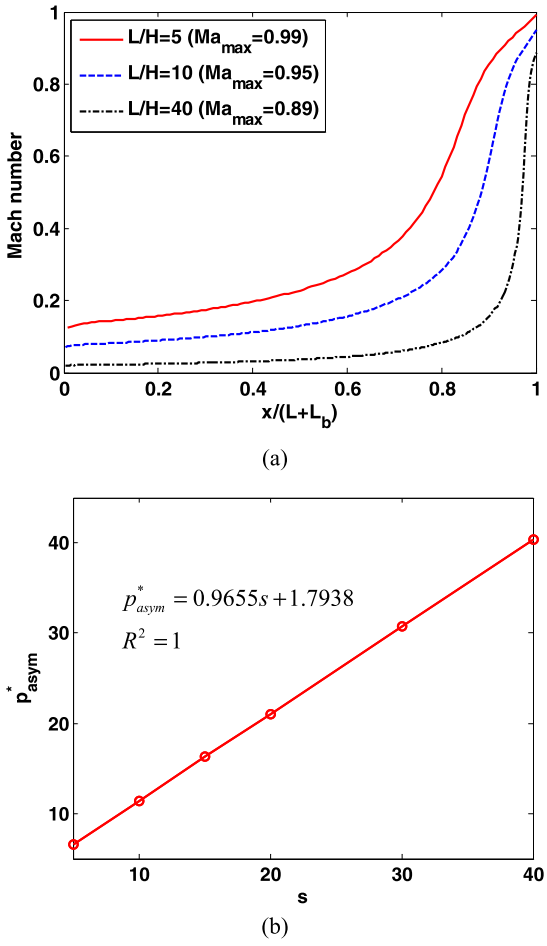

Fig. 5. (a) Mach number distributions of choked gas flows along the centerline of the channel for different lengths at $p_i' = 0.1$ MPa. (b) Asymptotical effective pressure ratio p^*_{asym} changes with the length height ratio s of microchannel. The open circles are simulation results and the straight line is a reference line. The fitting linear equations and the coefficient of determination are shown in the figure.

4. Conclusions

In this work, we studied the mechanism of choked gas flows in straight microchannels using the generalized Enskog Monte Carlo (GEMC) method. Our results are concluded as follows. (i) Numerical simulations indicate that the sonic point does not always appear even though the gas flows are choked in microchannels. It depends on the inlet–outlet pressure ratio and the length–height ratio of the channel. (ii) The choked gas flows in microchannel can be divided into two types: sonic choking and subsonic choking. (iii) The effective pressure ratio (p_i/p_o) really acting on the channel becomes asymptotically changeless when the given pressure ratio on the buffer regions (p_i'/p_o') is higher than a certain value. The subsonic choking may caused by the expansion wave or the strong non-equilibrium effect at the outlet of channel. (iv) The asymptotical value of p_i/p_o also depends on the inlet pressure and geometrical information of channel. For a choked gas flows with a given inlet pressure, the asymptotical effective pressure ratio may vary linearly with the length–height ratio.

Conflict of interest statement

Competing financial interests: The authors declare no competing financial interests.

Acknowledgements

This work is financially supported by the NSF grants of China (Nos. 51176089, 51321002), the Key Basic Scientific Research Program (2013CB228301) and the Tsinghua University Initiative Scientific Research Program (No. 2014z22074).

References

[1] G.M. Whitesides, The origins and the future of microfluidics, Nature 442 (2006) 368–373.
[2] J. Kobayashi, Y. Mori, K. Okamoto, R. Akiyama, M. Ueno, T. Kitamori, S. Kobayashi, A microfluidic device for conducting gas–liquid–solid hydrogenation reactions, Science 304 (2004) 1305–1308.
[3] G. Karniadakis, A. Beskok, N. Aluru, Microflows and Nanoflows: Fundamentals and Simulation, Springer, New York, 2005.
[4] S. Kandlikar, S. Garimella, D.Q. Li, S. Colin, M. King, Heat Transfer and Fluid Flow in Minichannels and Microchannels, Elsevier, Waltham, 2014.
[5] M. Wang, Z.X. Li, Numerical simulations on performance of MEMS-based nozzles at moderate or low temperatures, Microfluid. Nanofluid. 1 (2004) 62–70.
[6] P.F. Hao, Y.T. Ding, Z.H. Yao, F. He, K.Q. Zhu, Size effect on gas flow in mciro nozzles, J. Micromech. Microeng. 15 (2005) 2069–2073.
[7] M. Darbandi, E. Roohi, Study of subsonic–supersonic gas flow through micro/nanoscale nozzles using unstructured DSMC solver, Microfluid. Nanofluid. 10 (2011) 321–335.
[8] K.D. Wise, Integrated sensors, MEMS, and microsystems: reflections on a fantastic voyage, Sens. Actuators A, Phys. 136 (2007) 39–50.
[9] G.L. Morini, Y. Yang, H. Chalabi, M. Lorenzini, A critical review of the measurement techniques for the analysis of gas microflows through microchannels, Exp. Therm. Fluid Sci. 35 (2011) 849–865.
[10] B. Ding, M.R. Wang, J.Y. Yu, G. Sun, Gas sensors based on electrospun nanofibers, Sensors 9 (2009) 1609–1624.
[11] X.L. Zhang, L. Xiao, X.W. Shan, L. Guo, Lattice Boltzmann simulation of shale gas transport in organic nano-pores, Sci. Rep. 4 (2014) 4843.
[12] C.M. Freeman, G.J. Moridis, T.A. Blasingame, A numerical study of microscale flow behavior in tight gas and shale gas reservoir systems, Transp. Porous Media 90 (2011) 253–268.
[13] W.W. Liou, Y.C. Fang, Heat transfer in microchannel devices using DSMC, J. Microelectromech. Syst. 10 (2001) 274–279.
[14] E.B. Arkilic, K.S. Breuer, M.A. Schmidt, Mass flow and tangential momentum accommodation in silicon micromachined channels, J. Fluid Mech. 437 (2001) 29–43.
[15] T. Araki, M.S. Kim, H. Iwai, An experimental investigation of gaseous flow characteristics in microchannels, Microscale Thermophys. Eng. 6 (2002) 117–130.
[16] M. Wang, Z.X. Li, Nonideal gas flow and heat transfer in micro- and nanochannels using the direct simulation Monte Carlo method, Phys. Rev. E 68 (2003) 046704.
[17] Z.H. Yao, F. He, Y. Ding, M. Shen, X. Wang, Low-speed gas flow subchoking phenomenon in a long-constant-area microchannel, AIAA J. 42 (2004) 1517–1521.
[18] N. Dongari, A. Agrawal, A. Agrawal, Analytical solution of gaseous slip flow in long microchannels, Int. J. Heat Mass Transf. 50 (2007) 3411–3421.
[19] U. Kursun, J.S. Kapat, Modeling of microscale gas flows in transition regime, part I: flow over backward facing steps, Nanoscale Microscale Thermophys. Eng. 11 (2007) 15–30.
[20] S.P. Mahulikar, H. Herwig, O. Hausner, Study of gas microconvection for synthesis of rarefaction and nonrarefaction effects, J. Microelectromech. Syst. 16 (2007) 1543–1556.
[21] M. Le, I. Hassan, N. Esmail, The effects of outlet boundary conditions on simulating supersonic microchannel flows using DSMC, Appl. Therm. Eng. 27 (2007) 21–30.
[22] M. Wang, X.D. Lan, Z.X. Li, Analyses of gas flows in micro- and nanochannels, Int. J. Heat Mass Transf. 51 (2008) 3630–3641.
[23] A. Agrawal, A comprehensive review on gas flow in microchannels, Int. J. Micro-Nano Scale Transp. 2 (2011) 1–40.
[24] H. Shokouhmand, S. Bigham, R.N. Isfahani, Effects of Knudsen number and geometry on gaseous flow and heat transfer in a constricted microchannel, Heat Mass Transf. 47 (2011) 119–130.
[25] S. Colin, Gas microflows in the slip flow regime: a critical review on convective heat transfer, J. Heat Transf. 134 (2012) 020908.
[26] W.M. Zhang, G. Meng, X. Wei, A review on slip models for gas microflows, Microfluid. Nanofluid. 13 (2012) 845–882.
[27] C. White, M.K. Borg, T.J. Scanlon, J.M. Reese, A DSMC investigation of gas flows in micro-channels with bends, Comput. Fluids 71 (2013) 261–271.
[28] C. Cai, Surface stagnation point properties for highly rarefied planar jet impingement flow, Phys. Fluids 25 (2013) 106103.
[29] X.D. Shan, M. Wang, Effective resistance of gas flow in microchannels, Adv. Mech. Eng. 2013 (2013) 950681.

[30] M. Wang, Z.X. Li, Similarity of ideal gas flow at different scales, Sci. China Ser. E 46 (2003) 661–670.
[31] F.M. White, Fluids Mechanics, WCB McGraw–Hill, New York, 2011.
[32] E. Roohi, M. Darbandi, V. Mirjalili, DSMC solution of supersonic scale to choked subsonic flow in micro to nano channels, in: Proceedings of the 6th International Conference on Nanochannels, Microchannels, and Minichannels, Pts A and B, 2008, pp. 985–993.
[33] C. Xie, Subsonic choked flow in the microchannel, Phys. Fluids 18 (2006) 127104.
[34] M. Wang, Z.X. Li, An Enskog based Monte Carlo method for high Knudsen number non-ideal gas flows, Comput. Fluids 36 (2007) 1291–1297.
[35] D.B. Hash, J.N. Moss, H.A. Hassan, Direct simulation of diatomic gases using the generalized hard-sphere model, J. Thermophys. Heat Transf. 8 (1994) 758–764.
[36] J. Fan, A generalized soft-sphere model for Monte Carlo simulation, Phys. Fluids 14 (2002) 4399–4405.
[37] M. Wang, Z.X. Li, Gas mixing in microchannels using the direct simulation Monte Carlo method, Int. J. Heat Mass Transf. 49 (2006) 1696–1702.
[38] M.R. Wang, Z.X. Li, Simulations for gas flows in microgeometries using the direct simulation Monte Carlo method, Int. J. Heat Fluid Flow 25 (2004) 975–985.
[39] P.C. Malte, K.R. Sivier, Experimental evaluation of a subsonic expansion tube, in: A.A. Mich (Ed.), National Aeronautics and Space Administration, Washington, DC, 1969.
[40] V. Varade, A. Agrawal, A.M. Pradeep, Experimental study of rarefied gas flow near sudden contraction junction of a tube, Phys. Fluids 26.
[41] V. Varade, A. Agrawal, A.M. Pradeep, Behaviour of rarefied gas flow near the junction of a suddenly expanding tube, J. Fluid Mech. 739, 363–391.